Chapter 7

Development and On-Orbit Demonstration of Lithium-Ion Capacitor-Based Power System for Small Spacecraft

Masatoshi Uno and Akio Kukita

Additional information is available at the end of the chapter

http://dx.doi.org/10.5772/64966

Abstract

Lithium-ion capacitors (LICs) offer higher energy density and specific energy than do traditional electric double-layer capacitors (EDLCs). In spacecraft power systems where traditional lithium-ion batteries (LIBs) have been used with shallow depth of discharge (DoD) in order to achieve long-cycle life, LICs would potentially be an alternative to secondary batteries. Firstly, this chapter presents the quantitative comparison between the LIB- and LIC-based spacecraft power system from the viewpoint of system mass. On the basis of the potential suggested by the comparison, we have been developing the technology demonstration platform named "NESSIE" that contains the LIC pouch cell as one of its major demonstration missions. NESSIE was successfully launched with the main satellite HISAKI on September 2013. This chapter also presents the development of the LIC pouch cell for NESSIE and its experimental (or ground test) and on-orbit operation data.

Keywords: cycle life testing, lithium-ion capacitor, pouch cell, spacecraft power system, vacuum tolerance

1. Introduction

Applications of secondary battery-based energy storage are rapidly expanding from portable electronic devices to large-scale systems, including electric vehicles and grid-connected applications. Among various secondary battery chemistries, lithium-ion batteries (LIBs) are the most promising and viable for portable and vehicular applications thanks to their highest energy density and specific energy. Vigorous research and development efforts for increased energy density and extended service life are underway.

Meanwhile, supercapacitors (SCs), formally known as electric double-layer capacitors (EDLCs), are also an attractive energy storage device that plays an important role in various scenes. Thanks to their energy storage mechanism utilizing the double-layer capacitance on porous-activated carbon electrodes, EDLCs offer remarkable advantages over traditional secondary batteries in terms of cycle life, power capability, safety, and allowable temperature range. However, their low-energy density property is generally considered as a major drawback to be used as an alternative energy storage source to traditional secondary batteries. Hence, applications of EDLCs are chiefly limited to hybrid energy storage applications where EDLCs play a role of the high-power energy buffer that complements the main energy sources, such as secondary batteries and fuel cells.

To cope with the drawback of the low-energy density of EDLCs, lithium-ion capacitors (LICs) have been developed and commercialized by several manufacturers. LICs are basically a hybrid electrochemical capacitor combining double-layer capacitance and lithium intercalation for energy storage mechanism, and they offer the higher specific energy than EDLC without sacrificing the major benefits of EDLCs. LICs have been drawing significant attentions in vehicular and industry applications where high-power energy buffers are indispensable. Despite the increased energy density property, there is still a huge gap between LICs and secondary batteries.

Figure 1. EDLC-based uninterruptible power supplies (UPSs).

However, once the excellent long-cycle life performance of EDLCs and LICs is factored in, it drives expectation that EDLCs and LICs would be an alternative energy storage source to traditional secondary batteries in certain applications. For example, EDLC-based uninterruptible power supplies (UPSs) have been commercialized [1], as shown in **Figure 1**, as maintenance-free alternatives aiming for infrastructure applications where traditional lead-acid

http://dx.doi.org/10.5772/64966

batteries need to be replaced with new ones for every few years. Another potential application is a spacecraft power system where long-life energy storage sources are essential. In the previous study [2, 3], systematic cycle life testing emulating low-Earth-orbit (LEO) satellite conditions has been performed for EDLCs and LICs, and the results demonstrated that excellent cycle life performance can be expected for cycling conditions for LEO satellites.

For spacecraft applications where specific energy is of great importance, LICs are undoubtedly superior to EDLCs. Despite the great potential suggested in the laboratory cycle life testing, LICs had not been used in practical space applications. In order to demonstrate the LIC performance in practical on-orbit conditions, we developed the technology demonstration platform named 'NESSIE (NExt-generation Small Satellite Instrument for Electric power systems)' containing an LIC pouch cell as one of its major components to be demonstrated on orbit; NESSIE's major missions are (1) on-orbit demonstration for the LIC cells and (2) on-orbit demonstration for high-efficiency thin-film solar cells. NESSIE was embedded in the main satellite named "HISAKI", the Spectroscopic Planet Observatory for Recognition of Interaction of Atmosphere (see **Figure 2**) and was launched on September 14, 2013.

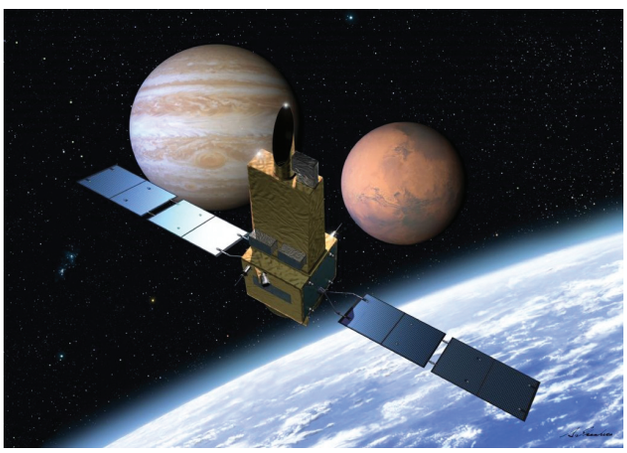

Figure 2. An image of HISAKI.

In this chapter, the quantitative comparison between LIB- and LIC-based spacecraft power systems is performed in terms of system mass. This chapter also presents the development of the LIC pouch cell for NESSIE and its experimental (or ground test) and on-orbit operation data.

2. Cycle life of LICs

In the previous study [4], cycle life testing emulating LEO spacecraft conditions was performed for LICs, and capacitance retentions of LICs were compared to those of LIBs under the same temperature conditions, as shown in **Figure 3**. The capacitance retention of the LIB with the shallow DoD of 20% dropped to approximately 70% at 10,000 cycles, which is equivalent to approximately 2-year operation, while that of LICs was still greater than 95%.

Furthermore, different from LIBs whose retention trends were dependent on DoD, the LICs showed DoD-independent trends.

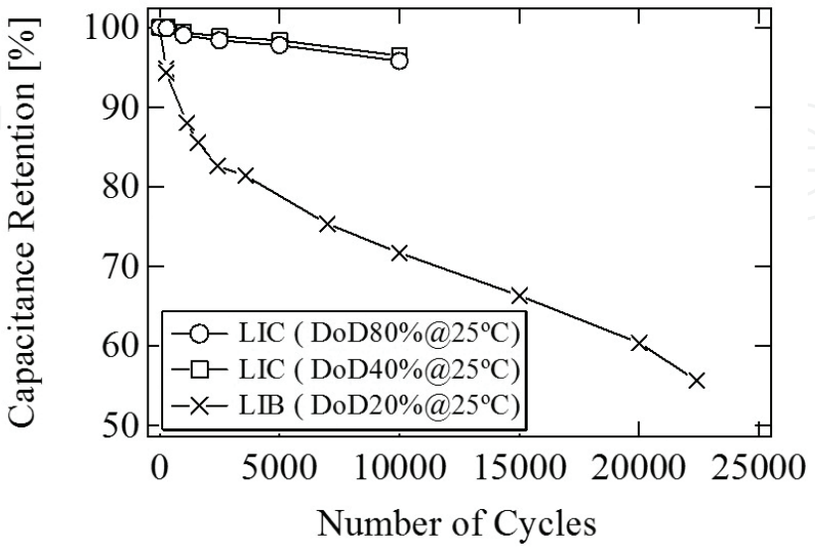

Figure 3. Capacitance retention trends of LIBs and LICs [4].

The accelerated ageing testing and the cycle life prediction model for LICs were also investigated in the previous study [3]. LIC cells were cycled at various temperatures in the systematically designed cycle test matrix. The activation energies of degradation ratios of LIC cells were calculated using the Arrhenius equation, whereupon ageing acceleration factors were determined. The experimental and predicted capacitance retention trends matched satisfactorily, and hence, the established cycle life prediction model was verified. According to the reported results in [3], LICs are expected to operate even longer than millions of cycles at temperature lower than 10°C.

The mission life of the main satellite HISAKI was 1 year, and therefore, the cycle life of LICs reported in the previous studies was adequate for NESSIE. However, the cycle life testing reported in the previous study was performed under laboratory conditions, leaving the investigation of tolerance against space environment, such as vacuum, vibration, and radiation, as issues to be cleared. Section 4 discusses these issues in detail.

3. LIC- and LIB-based power system comparison

3.1. Specific energy

Cycle life performance of traditional secondary batteries is greatly dependent on DoD. In general, secondary batteries for LEO satellites are operated with DoD shallower than 40% in

http://dx.doi.org/10.5772/64966

order to meet the typical cycle life requirement of 30,000 cycles that is equivalent to approximately 5.7 years on-orbit operation. In other words, the net specific energy of secondary batteries is far lower than their rated specific energy because of the shallow DoD operation. Specific energies as well as net specific energies of various energy storage devices are compared in **Table 1**. Although LIBs offer the highest specific energy of 150 Wh/kg, their net specific energy drops to as low as 60 Wh/kg with DoD of <40%.

	Secondary battery		**Capacitor**	
	Alkaline battery (Ni-Cd, Ni-MH, and Ni-H_2)	**Lithium-ion battery (LIB)**	**Electric double-layer capacitor (EDLC)**	**Lithium-ion capacitor (LIC)**
Specific energy	40–60 Wh/kg	150 Wh/kg	<10 Wh/kg	<30 Wh/kg
Depth of discharge	<40%	<40%	<80%	<80%
Net specific energy	<24 Wh/kg	<60 Wh/kg	<8 Wh/kg	<24 Wh/kg

Table 1. Specific energy and net specific energy of energy storage devices.

EDLCs and LICs, on the other hand, offer excellent cycle life performance that is insensitive to DoD conditions, allowing deep DoD operations. In the case of the 80% DoD operation for EDLCs and LICs, for example, their net specific energies are <8 Wh/kg and <24 Wh/kg, respectively, greatly bridging the gap in terms of net specific energy.

3.2. Photovoltaic array reduction by constant power charging scheme

A charging profiles of a 10-Wh LIB cell with a constant-current-constant-voltage (CC-CV) charging scheme are shown in **Figure 4(a)** as typical characteristics. The charging power peaks at the end of the CC charging period (or at the beginning of the CV charging period), when both the current and voltage become maximum. The chargeable state of charge (SoC) in the CC charging period is merely 60%, and the rest 40% is charged with CV charging. This characteristic indicates that the CV charging is indispensable for LIBs to reach high SoC. In typical LEO satellites, photovoltaic (PV) arrays are designed to be capable of supplying not only load power but also this peak charging power.

Different from LIBs mentioned above, LICs and EDLCs can be charged to nearly 100% SoC without CV charging because of their low-impedance properties. A charging profiles of a 10-Wh LIC cell with the constant-power (CP) charging scheme, instead of CC-CV charging scheme, are shown in **Figure 4(b)**. The charging power with the CP charging scheme is constant, and its peak value is substantially lower than that with the CC-CV charging scheme. This reduction in peak charging power contributes to the reduction in area and mass of PV arrays, as will be exemplified in Section 3.6.

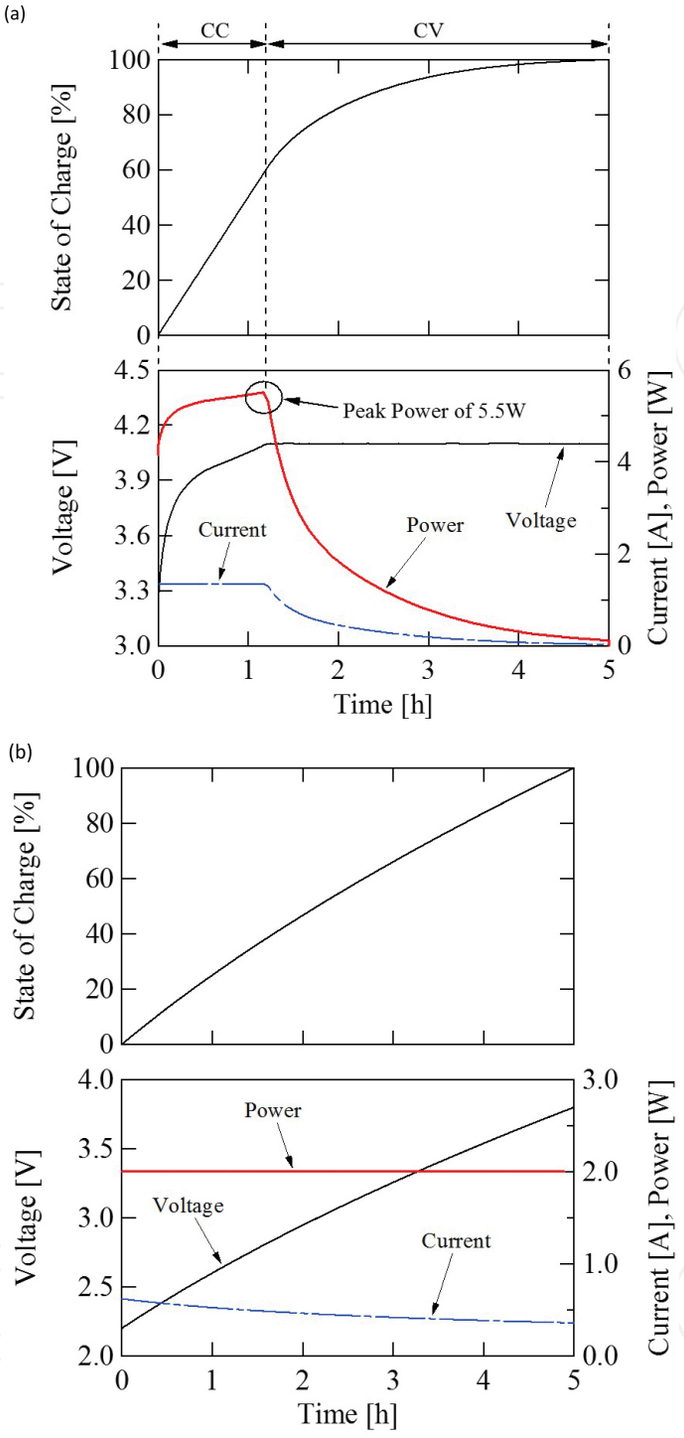

Figure 4. Comparison between (a) CC-CV charging and (b) CP charging schemes.

3.3. Power system using LIC

An unregulated bus system using an array power regulator (APR), as shown in **Figure 5(a)**, is mainstream for low- to medium-scale spacecraft power systems using an LIB-based energy storage. The LIB can be directory connected to the load (or bus) because of the relatively float

voltage characteristics. The APR plays a role of battery charging, and a load power is supplied by the LIB and/or APR.

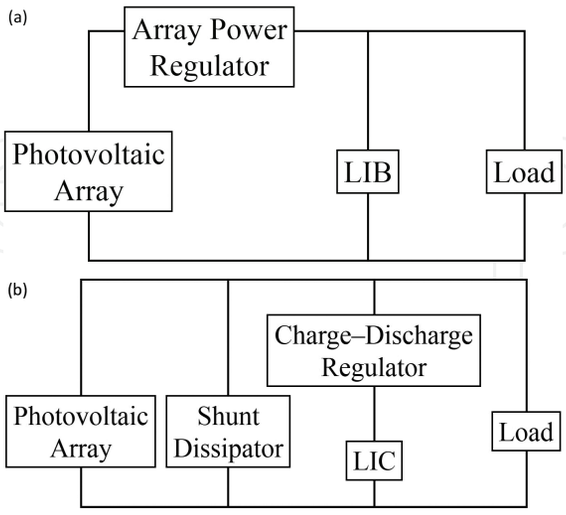

Figure 5. Spacecraft power system architectures for (a) LIB- and (b) LIC-based systems.

On the other hand, an LIC cannot be directory connected to the bus because of the relatively large-voltage variation (see **Figure 4(b)**), and therefore, a charge-discharge regulator (CDR) is necessary. An LIC-based power system using a shunt dissipator as a bus voltage regulator is shown in **Figure 5(b)**. In the following subsections, power systems shown in **Figure 5** are compared from the viewpoint of mass.

3.4. Mass of LIB-based power system

A single charge-discharge cycle consists of the sun and eclipse periods T_{sun} and T_{eclipse}, respectively. The discharged energy during the eclipse period E_{dis_LIB} is

$$E_{dis\_LIB} = P_{load} T_{eclipse} \tag{1}$$

where P_{load} is the load power.

Batteries contain not only cells but also mechanical structural support that represents nearly 20% increase in mass over that of cells. Now, the ratio of the mechanical support to cells is defined as A. The mass of the LIB, M_{LIB}, is expressed as

$$M_{LIB} = \frac{E_{dis\_LIB}(1+A)}{DS_{LIB\_cell}} \tag{2}$$

where D is the DoD, and S_{LIB_cell} is the specific energy of LIB cells.

Let V_{ave} be the average voltage of the LIB during discharging. The capacity of the LIB, C_{LIB}, can be determined as

$$C_{LIB} = \frac{E_{dis\_LIB}}{DV_{ave}} \tag{3}$$

Introducing the charge rate (also known as C-rate) as R_{cha}, the charge current for the LIB, I_{cha}, is yielded as

$$I_{cha} = C_{LIB} R_{cha} \tag{4}$$

The value of R_{cha} can be determined from the charge-discharge ratio that is defined as

$$R_{C/D} = \frac{R_{cha} T_{sun}}{D} \tag{5}$$

Generally, a typical value of $R_{C/D}$ for LEO spacecraft is 1.25 [5].

The maximum charging power (P_{cha_LIB}) at the end of the CC charging or at the beginning of the CV charging, at which the LIB voltage is as high as V_{cha}, is

$$P_{cha\_LIB} = V_{cha} I_{cha} \tag{6}$$

The mass of the PV arrays in the LIB-based power system, M_{PV_LIB}, can be determined to be

$$M_{PV\_LIB} = \frac{P_{load} + P_{cha\_LIB}}{\eta_{APR} \rho_{PV}} \tag{7}$$

where η_{APR} is the power conversion efficiency of the APR and ρ_{PV} is the specific power of the PV array.

The mass of the power conditioning system M_{PCS_LIB}, which is equal to the mass of the APR in the LIB-based power system, is expressed as

$$M_{PCS\_LIB} = m_{APR} \left(P_{cha\_LIB} + P_{load} \right) \tag{8}$$

where m_{APR} is the mass/watt coefficient of the APR.

From Eqs. (2), (7), and (8), the total mass of the LIB-based power system M_{LIB_system} is obtained as

$$M_{LIB\_system} = M_{LIB} + M_{PV\_LIB} + M_{PCS\_LIB} \tag{9}$$

3.5. Mass of LIC-based power system

Let η_{CDR} be the power conversion efficiency of the CDR. The discharged energy of the LIC E_{dis_LIC} can be expressed as

$$E_{dis\_LIC} = \frac{P_{load} T_{eclipse}}{\eta_{CDR}} \tag{10}$$

With the specific energy of the LIC cells S_{LIC_cell}, the mass of the LIC, M_{LIC}, can be represented as

$$M_{LIC} = \frac{E_{dis\_LIC}\left(1 + A\right)}{DS_{LIC\_cell}} \tag{11}$$

Assuming that the LIC is fully charged at the end of the sun period, the power demanded for the PV array from the LIC, P_{cha_LIC}, is expressed as

$$P_{cha\_LIC} = \frac{E_{dis\_LIC}}{\eta_{CDR} T_{sun}} \tag{12}$$

The mass of the PV arrays in the LIC-based power system, M_{PV_LIC}, is

$$M_{PV\_LIC} = \frac{P_{load} + P_{cha\_LIC}}{\rho_{PV}} \tag{13}$$

Assuming the shunt dissipator is designed to be capable of the sum of P_{load} and P_{cha_LIC}, the mass of the PCS in the LIC-based power system, M_{PCS_LIC}, is given by

$$M_{PCS\_LIC} = P_{load} m_{CDR} + m_{shunt}\left(P_{cha\_LIC} + P_{load}\right) \tag{14}$$

where m_{CDR} and m_{shunt} are the mass/watt coefficient of the CDR and shunt dissipator, respectively.

From Eqs. (11), (13), and (14), the total mass of the LIC-based power system M_{LIC_system} is determined as

$$M_{LIC\_system} = M_{LIC} + M_{PV\_LIC} + M_{PCS\_LIC} \tag{15}$$

3.6. System mass comparison

The LIB- and LIC-based power systems, shown in **Figure 5**, are quantitatively compared using the parameters listed in **Table 2**. These values were determined according to the literature [6].

Parameter	Symbol	Value
Load power	P_{load}	1000 W
Sun period	T_{sun}	1 h
Eclipse period	$T_{eclipse}$	0.5 h
C/D ratio (for LIB only)	$R_{C/D}$	1.25
Charge voltage (LIB only)	V_{cha}	28.7 V
Average discharge voltage (LIB only)	V_{ave}	25.9 V
Mass ratio of mechanical structural supports to cells	A	20%
Specific power of PV array	ρ_{PV}	60 W/kg
Efficiency of array power regulator	η_{APR}	90%
Efficiency of charge/discharge regulator	η_{CDR}	90%
Mass/watt coefficient of array power regulator	m_{APR}	4 kg/kW
Mass/watt coefficient of charge/discharge regulator	m_{CDR}	4 kg/kW
Mass/watt coefficient of shunt dissipator	m_{Shunt}	2 kg/kW

Table 2. Parameters used for mass comparison.

Figure 6 depicts the system mass of 1-kW LIB- and LIC-based power systems, with nominal specific energies (S_{LIB_cell} = 150 Wh/kg and S_{LIC_cell} = 30 Wh/kg) ±20% variation, as a function of DoD. As mentioned earlier, in order for LIBs to meet the typical cycle life requirement of 30,000 cycles, DoD should be set as shallow as 40% to mitigate cycling-induced degradation. The mass of the LIB-based power system with 40% DoD is around 50 kg and lighter than the LIC-based system, indicating the traditional LIB-based power system is superior for the typical 30,000-cycle life requirement from the viewpoint of system mass. For longer cycle life requirement, on the other hand, LIBs have to be cycled with even shallower DoD, and therefore, the mass of the LIB-based power system is prone to sharp increase, as can be found around 20% DoD in **Figure 6**. Hence, the LIB-based system with shallow DoD competes with the LIC-based system. The mass of the LIB-based system with DoD of 15%, for example, is around 70 kg and is comparable with that of the LIC-based system with 60% DoD.

http://dx.doi.org/10.5772/64966

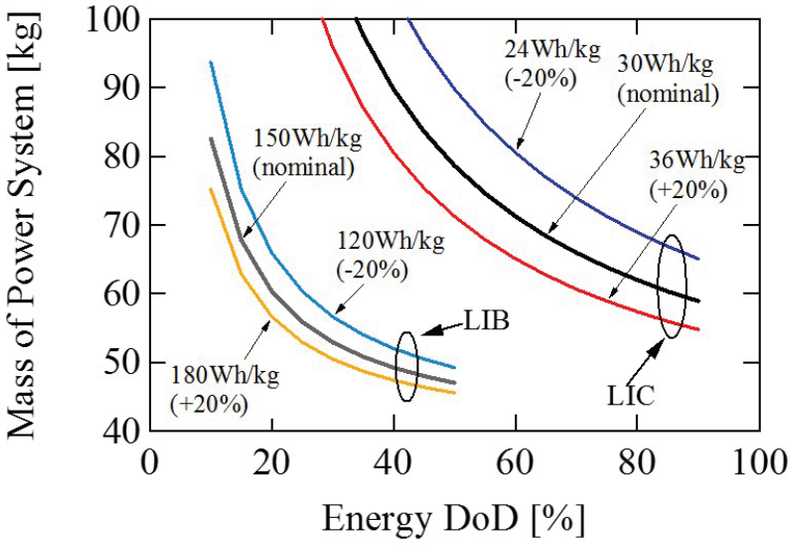

Figure 6. Mass of LIB- and LIC-based power systems as a function of DoD.

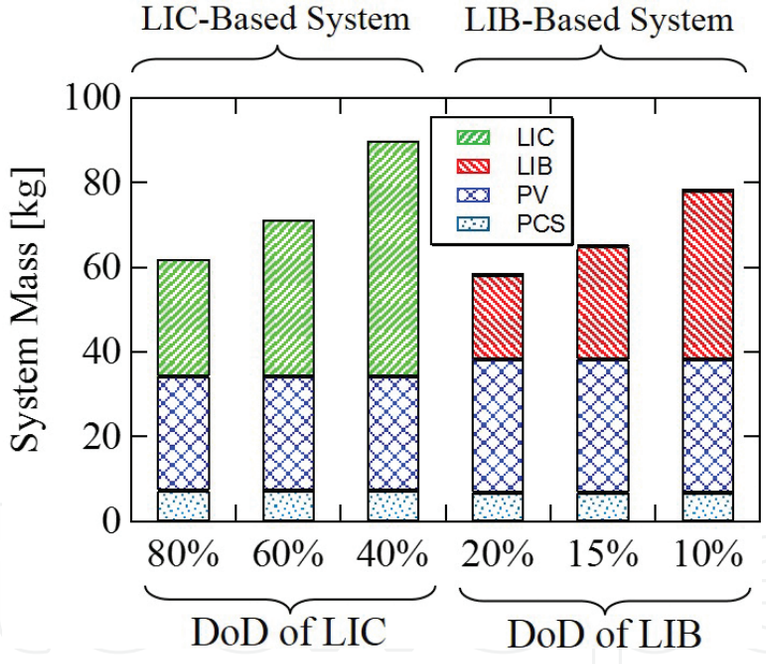

Figure 7. Mass breakdown of LIB- and LIC-based power systems.

The mass breakdown of the LIB- and LIC-based power systems with the nominal specific energies of S_{LIB_cell} = 150 Wh/kg and S_{LIC_cell} = 30 Wh/kg are compared in **Figure 7**. In the LIC-based power systems, the LIC accounted for greater than half the total mass of the systems. Meanwhile, thanks to the CP charging scheme introduced in Section 3.2, the mass of the PV array in the LIC-based system can be reduced compared to that in the LIB-based system. The total mass of the LIC-based system with DoD of 60–80% is comparable with that of LIB-based system with DoD of 15–20%, suggesting that LICs would be an alternative energy storage

source to LIBs for applications needing long-cycle life. Other benefits, such as wider operational temperature range of LICs, would further improve the likelihood of LICs being an alternative to traditional LIBs.

4. Development of LIC for NESSIE

4.1. Vacuum tolerance of LIC pouch cell

Needless to say, there is no air in the space, and therefore, components for spacecraft must be vacuum-tolerant. In general, secondary batteries for spacecraft power systems are reinforced by metal-housing so as to increase the ruggedness for shock and vibration during launch and tolerance against vacuum in space. In the previous developmental work, electrical characteristics of lithium-ion pouch cells were investigated [7]. The cells swelled in vacuum, and the performance of LIB pouch cells significantly deteriorated. In order to improve the vacuum tolerance, LIB pouch cells were potted with epoxy resin in an aluminium-housing. However, this reinforcement adversely increases the mass and volume of the battery, resulting in decreased specific energy, and it neutralizes the benefit of pouch cells of high specific energy.

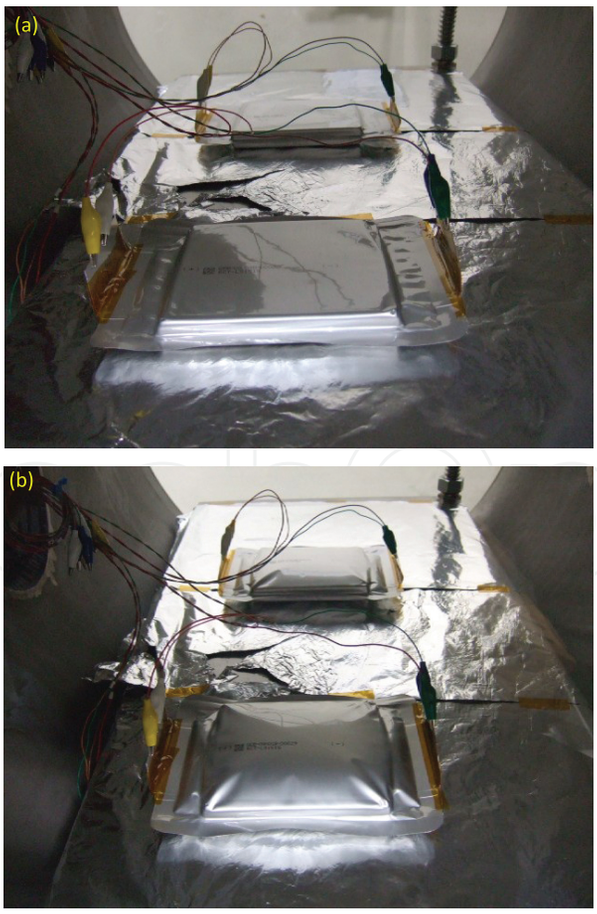

Figure 8. LIC pouch cells under (a) normal pressure and (b) vacuum.

http://dx.doi.org/10.5772/64966

Although both the resin- and metal-housing-based reinforcement were reportedly necessary for LIB pouch cells, we considered it was worth investigating whether LIC pouch cells work well in vacuum. To investigate vacuum tolerance of LIC pouch cells, we performed short-term cycle life testing for two LIC pouch cells in a vacuum chamber. In the vacuum chamber, LIC pouch cells were placed on a thermostatic plate that was controlled to be 25°C by a coolant circulator (see **Figure 8**). As reference data, the same cycling test under a normal pressure condition was also carried out for other two LIC pouch cells. A single charge-discharge cycle consists of 65-min CP charging and 35-min CC discharging with 80% DoD.

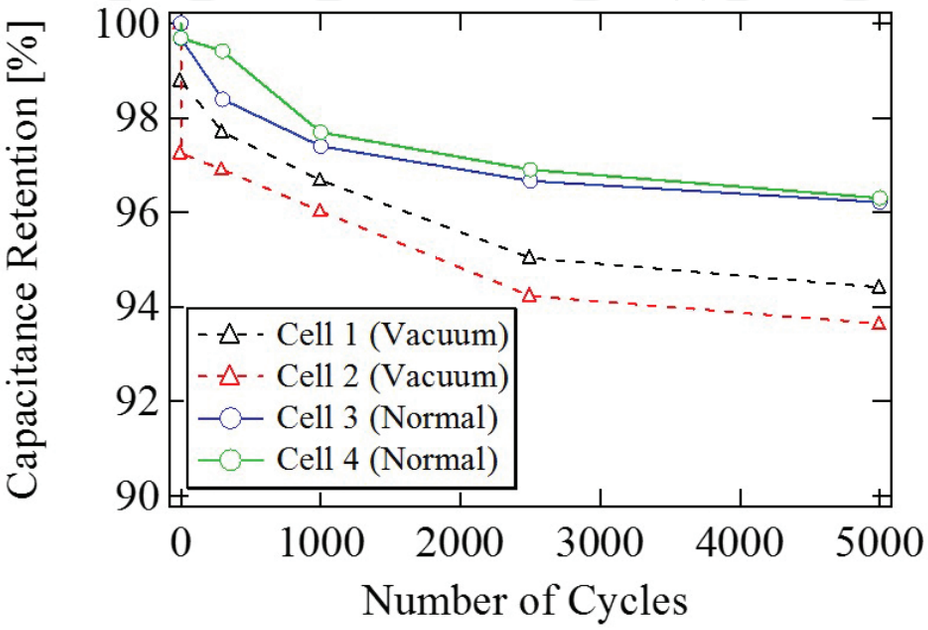

Figure 9. Capacitance retention trends of LICs cycled under normal pressure and vacuum conditions.

The pouch cells under normal pressure and vacuum are shown in **Figure 8(a)** and **(b)**, respectively. The LIC pouch cells swelled similarly to the LIB pouch cells reported in [7]. In spite of the significant shape deformation, the observed deterioration of cells in a vacuum was merely around 2%, compared to those under normal pressure, as shown in **Figure 9**. The capacitance retentions of cells dropped as the vacuum chamber was evacuated at the beginning of the testing (i.e., at an initial cycle). After this initial drop in capacitance retention, all cells exhibited the similar degradation trends. The measured capacitance retentions of cells in vacuum and under normal pressure at 5000th cycle (equivalent to 1-year on-orbit operation) were approximately 94 and 96%, respectively. **Figure 10** shows the discharge curve trends of LICs during capacitance measurement. The dischargeable time gradually shortened as cells deteriorated. However, no significant voltage decline due to an increase in internal resistance was observed, indicating that the vacuum condition did not increase an internal resistance of LIC pouch cells. The results shown in **Figures 9** and **10** suggested that bulky and heavy reinforcement using resin and/or metal-housing would not be mandatory even though pouch cells swelled.

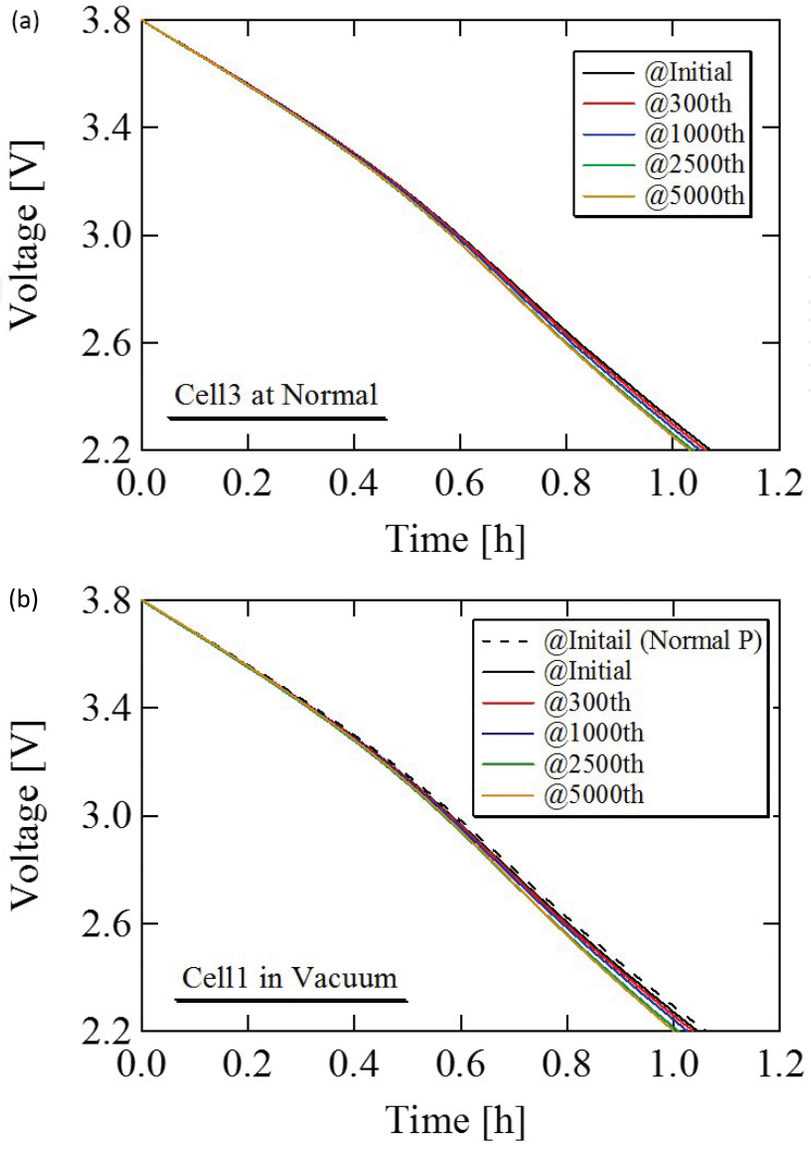

Figure 10. Discharge curve trends of LICs cycled under (a) normal pressure and (b) vacuum.

4.2. LIC pouch cell for NESSIE

NESSIE is a small demonstration platform, in which only one single LIC cell is allowed to be equipped. In general, for practical use, a plastic or metal container is used for pouch cells to be stacked and bundled to form a module. However, to reduce the mass of NESSIE, a container for the LIC pouch cell should be as simple and light as possible. In addition, although the results shown in **Figures 9** and **10** implied that LIC cells might be used without reinforcement, the swelling should be avoided because it might cause unexpected interference with other components in NESSIE. To prevent the swelling at the lightest possible measure, we developed a dedicated metal-bracket that looks 'III-shape', as shown in **Figure 11**. This metal bracket can suppress the swelling at a light mass. This LIC pouch cell with the metal bracket successfully passed the vibration test. The specification of the LIC cell for NESSIE is shown in **Table 3**.

http://dx.doi.org/10.5772/64966

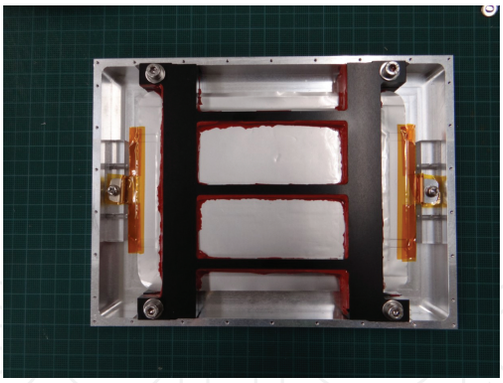

Figure 11. LIC cell with metal bracket.

Mass	303 g (bare cell)
	832 g (w/metal bracket)
Dimension	123 × 165 × 15 mm (bare cell)
	164 × 220 × 23 mm (w/metal bracket)
Manufacture	Asahikasei FDK energy device
Capacitance	2500 F

Table 3. Specification of LIC cell.

5. Development of NESSIE

5.1. Charge-discharge regulator for LIC

The LIC cell is charged and discharged by a CDR that is basically a bidirectional dc-dc converter. As explained in the previous section, LIC cells for the short-term cycle life testing in the vacuum chamber were charged and discharged with the CP charging and CC discharging schemes, respectively. In practical use, the bidirectional dc-dc converter plays the role of these charging and discharging schemes.

In general, a discharging power is simply determined by loads, and the bidirectional converter operates to regulate a load voltage at a constant value (e.g., 5 V in the NESSIE's power system). On the other hand, a charging power is controlled by the bidirectional converter based on measured voltage and current. To this end, a feedback control loop including current and voltage sensors is necessary. Furthermore, the measured current and voltage values need to be multiplied to determine the charging power. In general, for small-scale systems such as NESSIE, both circuit- and system-level simplifications are of great importance to realize the miniaturized circuit and system. In other words, the current and voltage sensors as well as computational circuit for determining the charging power are desirably be eliminated from the system.

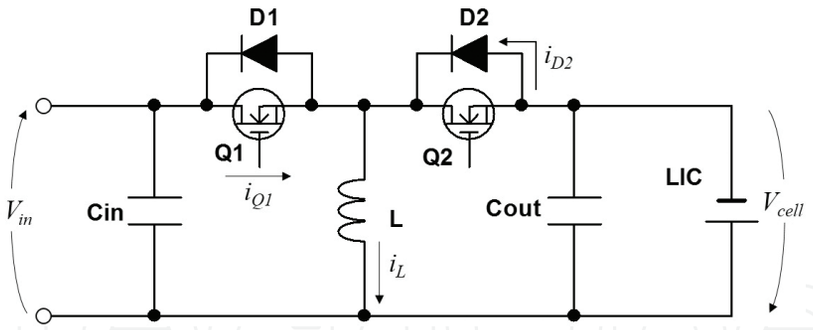

Figure 12. Bidirectional buck-boost converter as charge-discharge regulator for LIC.

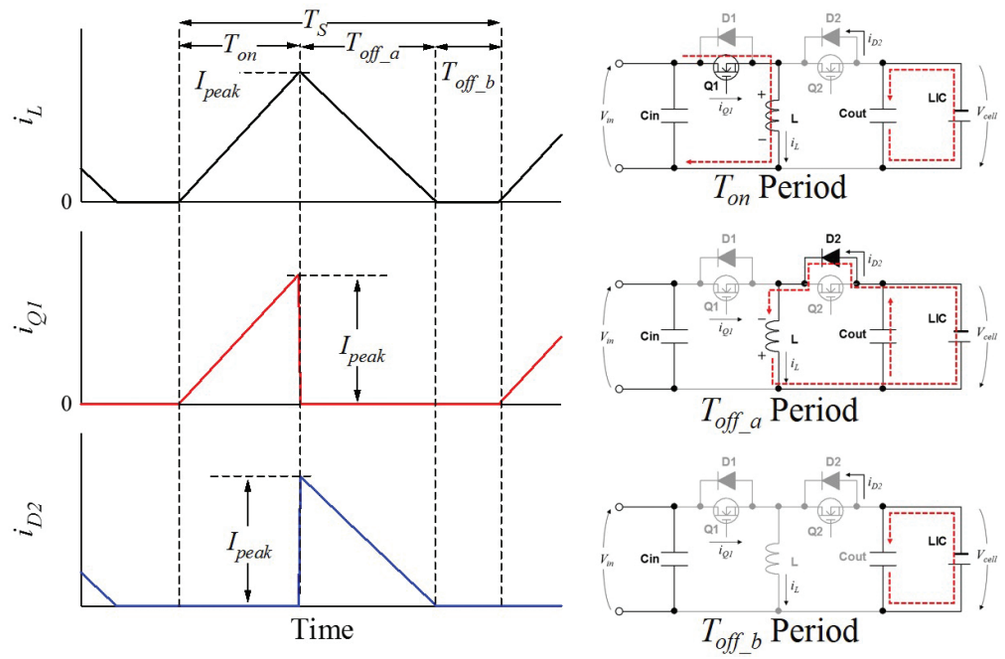

Figure 13. Key operation waveforms and current flow directions in DCM operation.

As a simplest possible solution, we employed a bidirectional buck-boost converter operating in the discontinuous conduction mode (DCM), with which the charging power can be automatically constant even without feedback control nor calculation of product of current and voltage. The bidirectional buck-boost converter and its key operation waveforms as well as current flow directions in DCM are shown in **Figures 12** and **13**, respectively. Switches Q_1 and Q_2 are driven so that an LIC is charged and discharged, respectively. The fundamental operation of the buck-boost converter is well known and can be found in basic textbooks, and hence, this subsection focuses on the mechanism of the CP charging. One switching cycle contains three modes, and T_{off_b} period, during which no current flows in the converter, is unique to DCM operation; the inductor current i_L reaches zero in the T_{off_b} period for every switching cycle. In this chapter, the operation for charging only is explained to save page length. To charge an LIC with the buck-boost converter shown in **Figure 12**, the switch Q_1 is

http://dx.doi.org/10.5772/64966

driven while Q_2 is always off. For discharging, on the other hand, the operation is vice versa —Q_2 is driven, and Q_1 is always off.

In the first mode, T_{on} period, i_L increases linearly from zero, and its inclination is equal to V_{in}/L. At the end of this mode, i_L reaches its peak value of I_{peak} expressed as

$$I_{peak} = \frac{V_{in} T_{on}}{L} = \frac{V_{in} D T_S}{L} \tag{16}$$

where T_S is the switching period and D is the duty cycle defined as T_{on}/T_S.

As Q_1 is turned off, the operation moves to T_{off_a} period, during which i_L linearly decreases from I_{peak} with the slope of $-V_{cell}/L$. i_L starts flowing through diode D_2 that is connected in parallel with Q_2. The time length of this period, T_{off_a}, can be determined to be

$$T_{off\_a} = I_{peak} \frac{L}{V_{cell}} = \frac{V_{in} D T_S}{V_{cell}} \tag{17}$$

As i_L reaches zero, the final mode of T_{off_b} period begins. In this mode, except for the current of the smoothing capacitor C_{out}, no current flows in the converter.

In order for T_{off_b} period to exist, T_{off_a} must be shorter than $T_S - T_{on}$, meaning $T_{off\_a} < T_S - T_{on}$. It leads to the operation criterion given by

$$D < \frac{V_{cell}}{V_{in} + V_{cell}} \tag{18}$$

The input current for the buck-boost converter is supplied only during T_{on} period, and hence, the input power (or charging power) can be expressed as

$$P_{in} = V_{in} \frac{I_{peak}}{2} \frac{T_{on}}{T_S} \tag{19}$$

This equation indicates that, with a constant on-time of T_{on}, the charging power for the LIC cell or P_{in} for the buck-boost converter can be automatically constant even without feedback control. In other words, open-loop control is feasible, hence allowing simplified control circuit.

The photograph of a power control unit (PCU) that contains the buck-boost converter is shown in **Figure 14**. The converter operated with a fixed D of 0.35 at a switching frequency of 100 kHz for the charging power to be approximately 3.8 W. For discharging periods, on the other hand, D was adjusted so that the load voltage was controlled to be 5.0 V.

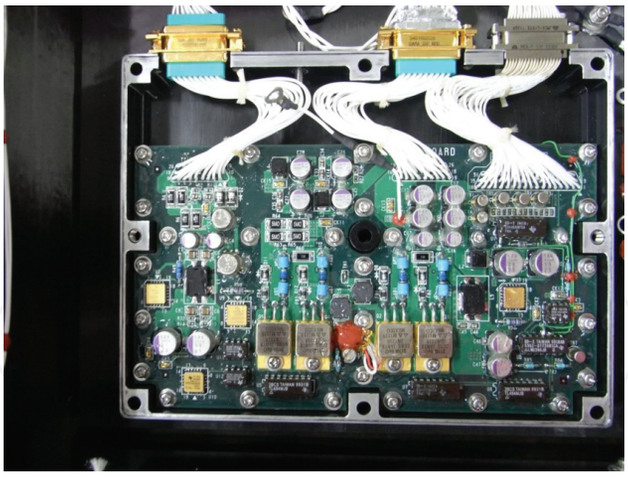

Figure 14. Photograph of power control unit (PCU) containing charge-discharge regulator.

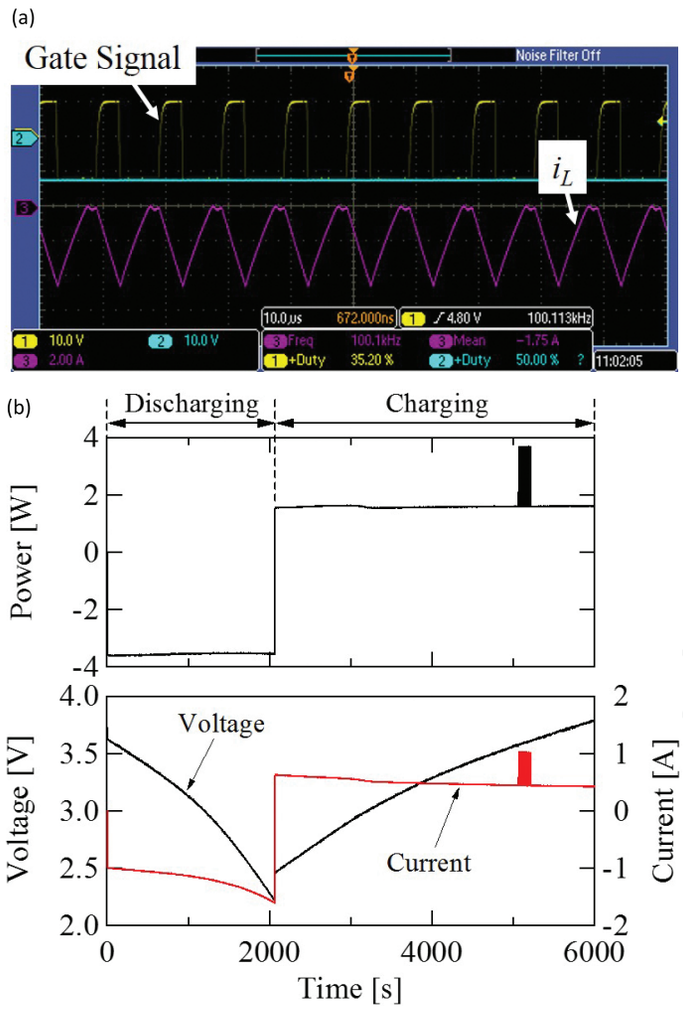

Figure 15. (a) Measured key operation waveforms of the buck-boost converter and (b) cycling profiles of an LIC cycled by the buck-boost converter.

http://dx.doi.org/10.5772/64966

The measured key operation waveforms during charging are shown in **Figure 15(a)**. The inductor current i_L swung as the gate signal for Q_1 was applied. The measured i_L was discontinuous triangular wave—the displayed i_L is inverted—and the good agreement with the theoretical ones was observed. A single charge-discharge cycling profile of an LIC cell with the buck-boost converter operating in DCM is shown in **Figure 15(b)**. The measured power during charging was nearly constant, verifying the automatic CP charging property.

5.2. NESSIE

The specification of NESSIE is listed in **Table 4**. The photographs of NESSIE installed in the main satellite HISAKI are shown in **Figure 16**. The high-efficiency thin-film solar cells were mounted on the main panel that was used as a lid for the interior components, including the LIC pouch cell and charge-discharge regulator. NESSIE was installed in the side panel of the main satellite HISAKI.

Mass	10.03 kg
Dimension	550 × 463 × 205 mm
Bus	5-V fully regulated
Power generation	>10 W (at end of life)

Table 4. Specification of NESSIE.

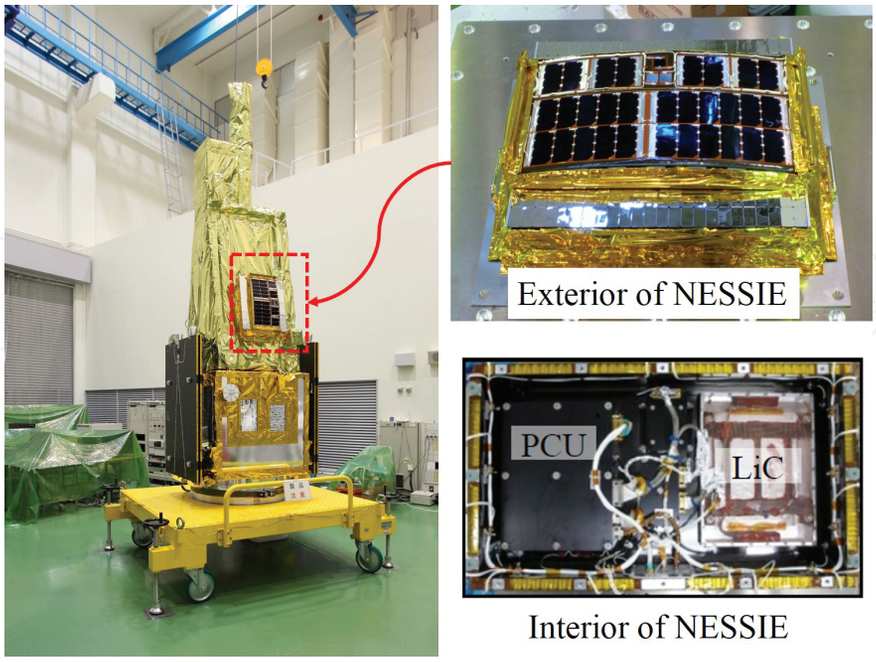

Figure 16. Photographs of NESSIE installed in HISAKI.

6. On-orbit operation

The main satellite HISAKI was launched by Epsilon-1 rocket on September 14, 2013, and NESSIE was turned on for the first time on October 12, 2013, and the LIC was cycled in the first check-up operation, as shown in **Figure 17**. During the first eclipse period, the LIC was nearly fully discharged to 2.2 V, followed by a CP charging during the subsequent sun period. The data at the beginning of the charging were temporarily not available because of an operation with low communication rate, with which essential housekeeping data for HISAKI only was acquired. The short-term pulsating discharges during charging periods were due to the measurement operation for the thin-film solar cells, during which the PV panel was short-circuited and the LIC supplied power to the loads. The first check-up results demonstrated the LIC as well as the charge-discharge regulator performed well.

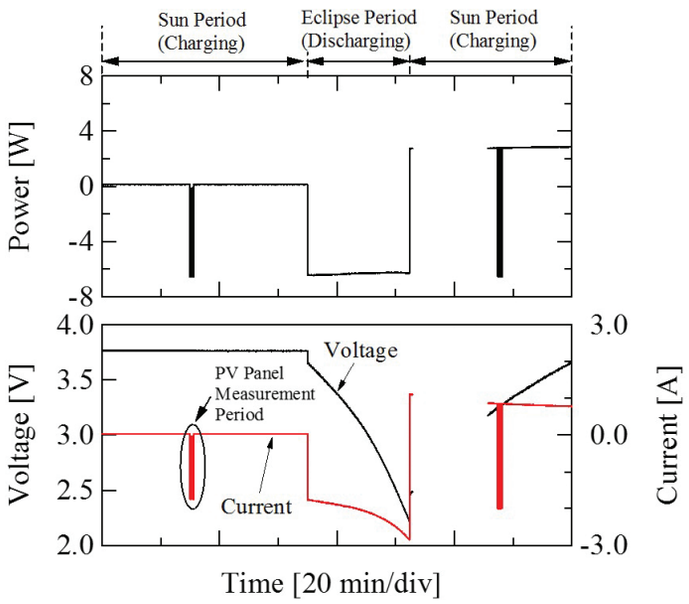

Figure 17. On-orbit cycling profiles during the first check-up.

Since approximately 1 month after the first check-up, the voltage of the PV panel of NESSIE has unexpectedly dropped. The decreased PV panel voltage was lower than the threshold voltage of the charge-discharge regulator. In other words, the voltage of the PV panel was not high enough for the charge-discharge regulator to operate, meaning the LIC has no longer been charged since then.

As the best effort we could do with the malfunctioning PV panel, we determined to turn on NESSIE only for a few minutes in every few months to observe the LIC pouch cell under the float condition. This is rather different from the originally planned cycling condition that was used for laboratory testing. But we consider that this floating operation of the LIC pouch cell would still be meaningful to demonstrate the on-orbit vacuum tolerance and to investigate whether unexpected malfunctions would happen to the LIC after long-term exposure to space environment.

http://dx.doi.org/10.5772/64966

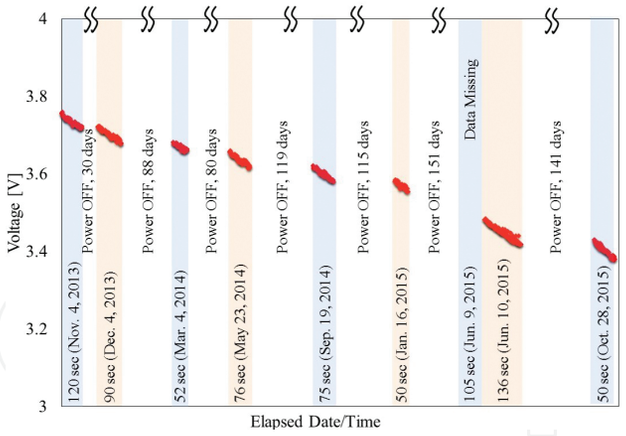

Figure 18. On-orbit trend of LIC voltage.

The trend of the LIC voltage is shown in **Figure 18**. As aforementioned, NESSIE was turned on for a few minutes in every few months, and the LIC-powered NESSIE and its voltage gradually decreased during the turn-on periods. During the turn-off periods, on the other hand, the voltage of the LIC unchanged as the voltages at the beginning and end of turn-off periods were nearly identical, indicating the insignificant self-discharge.

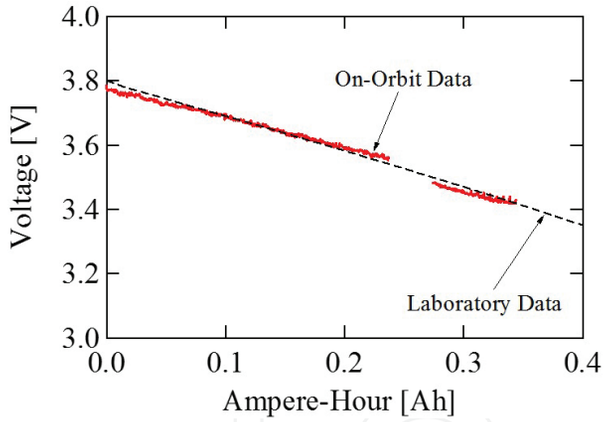

Figure 19. On-orbit trend of LIC voltage as a function of discharged ampere-hour capacity.

The on-orbit LIC's voltage trend shown in **Figure 18** is redrawn as a function of discharged capacity in ampere-hour and is compared to that of a cell tested in the laboratory, as shown in **Figure 19**. The on-orbit and laboratory data matched very well, suggesting the LIC has been performing well.

7. Conclusions

Although the specific energy of LICs is far lower than that of traditional LIBs, the gap between LICs and LIBs can be greatly bridged once long-cycle life performance with deep

DoD conditions is factored in. In addition, LICs allow the CP charging scheme, with which the mass of the PV panel can be reduced compared to that with a traditional CC-CV charging scheme. The mass of an LIC-based power system was compared to that of a LIB-based system. The results of the quantitative comparison suggested that, for applications requiring very long-cycle life, for which LIBs need to be cycled with DoD shallower than 20% to achieve long-cycle life, the LIC-based power system would be comparable to the LIB-based one, driving expectation that LIC would potentially be an alternative energy storage source.

We developed the technology demonstration platform named NESSIE whose one of the missions is the on-orbit demonstration of the LIC pouch cell. Short-term cycle life testing in vacuum was performed to investigate the vacuum tolerance of LIC pouch cells. The results of the 1-year testing suggested the deterioration in capacitance retention due to the vacuum condition was insignificant. The dedicated charge-discharge regulator, with which the LIC can be charged with the CP charging scheme even without feedback control, was also developed to realize simplified circuit.

NESSIE was launched with the main satellite HISAKI on September 14, 2013, and the first check-up data showed the successful charge-discharge cycling profiles of the LIC. However, the LIC has no longer been charged due to the malfunction of the PV panel since 1 month after the launch. Since then, as the best effort, the voltage trend of the LIC has been monitored to see whether long-term exposure to space environment has negative influence on the LIC. As of this writing, no malfunctioning trend has been observed, suggesting the LIC has still been performing well.

Author details

Masatoshi Uno[1*] and Akio Kukita[2]

*Address all correspondence to: masatoshi.uno.ee@vc.ibaraki.ac.jp

1 Ibaraki University, Hitachi, Japan

2 Japan Aerospace Exploration Agency, Sagamihara, Japan

References

[1] JCC. UPS-J EDLC Module [Internet]. Available from: http://www.jcc-foil.co.jp/cdg/products/index.html

[2] M. Uno and K. Tanaka. Accelerated charge-discharge cycling test and cycle life prediction model for supercapacitors in alternative battery applications. IEEE Transactions on Industry Electronics. 2012;59(12):4704–4712.

http://dx.doi.org/10.5772/64966

[3] M. Uno and A. Kukita. Cycle life evaluation based on accelerated aging testing for lithium-ion capacitors as alternative to rechargeable batteries. IEEE Transactions on Industry Electronics. 2016;63(3):1607–1617.

[4] M. Uno. Supercapacitor-Based Electrical Energy Storage System. InTech: Energy Storage in the Emerging Era of Smart Grids. 2011:21–44.

[5] X. Wang, Y. Sone, H. Naito, C. Yamada, G. Segami, and K. Kibe. Cycle-life testing of large-capacity lithium-ion cells in simulated satellite operation. Journal of Power Sources. 2006;161(1):594–600.

[6] M. Uno and K. Tanaka. Spacecraft electrical power system using lithium-ion capacitors. IEEE Transactions on Aerospace and Electronic Systems. 2013;49(1):175–188.

[7] M. Uno, K. Ogawa, Y. Takeda, Y. Sone, K. Tanaka, M. Mita, and H. Saito. Development and on-orbit operation of lithium-ion pouch battery for small scientific satellite "REIMEI". Journal of Power Sources. 2011;196(20):8755–8763.

IntechOpen